

Article

# Migration and Transformation of Ofloxacin by Free Chlorine in Water Distribution System

Weiwei Bi <sup>1</sup>, Yi Jin <sup>1</sup> and Hongyu Wang <sup>2,\*</sup>

<sup>1</sup> College of Civil Engineering and Architecture, Zhejiang University of Technology, Hangzhou 310023, China; weiweibi@zjut.edu.cn (W.B.); jinyizjut@sina.cn (Y.J.)

<sup>2</sup> College of Environment, Zhejiang University of Technology, Hangzhou 310023, China

\* Correspondence: whyzjut@163.com; Tel.: +86-571-8529-0520

Received: 8 March 2019; Accepted: 16 April 2019; Published: 19 April 2019



**Abstract:** This study investigated the degradation kinetics and product generation of ofloxacin (OFL) in the pipe network under different pipe materials, flow rate, pH, free chlorine concentration and temperature. The experiments done in the beaker and pipe network were compared. The results showed that the reaction rate of OFL chlorination with free chlorine increased with the increase of the free chlorine concentration in the pipe network and deionized water, and the degradation efficiency of OFL in the pipe network was higher than that in the deionized water, satisfying the second-order dynamics model. The degradation rate under different pHs was: neutral > acidic > alkaline. The influence of the flow rate is not significant while the influence of the pipe materials and temperature is obvious. The degradation rate of OFL increased with the increase of the temperature, indicating that the OFL degradation was an endothermic process. A liquid chromatograph-mass spectrometer (LC-MS) was used to detect the chlorination intermediates, and the results showed that the piperazine ring was the main group involved in the chlorination reaction, and the main point involved in the chlorination reaction was the N4 atom on the piperazine ring. We also found that, as the reaction time increases, the concentrations of trihalomethanes (THMs) and haloacetic acids (HAAs) increase and THMs mainly exist in the form of trichloromethane (TCM) while HAAs mainly exist in the form of monochloroacetic acid (MCAA).

**Keywords:** water distribution system; water quality; free chlorine; ofloxacin; degradation; kinetic study; formation mechanism

## 1. Introduction

In recent years, antibiotics and fluoroquinolones have been widely used in the treatment of various infectious diseases due to their broad antibacterial spectrum and strong efficacy [1–3]. However, as the use of these antibiotics and fluoroquinolones increases, some of them have been detected in the environment. This will affect the growth and development of the plant, and some of the microorganisms in the environment will have an inhibitory effect and may even be killed [4]. Ofloxacin (OFL) was used as the third generation of the fluoronone and has also been constantly detected in drinking water. Chlorine disinfection is the common method used to reduce OFL while the disinfection by-products, such as trihalomethanes (THMs) and haloacetic acids (HAAs), which have carcinogenic, teratogenic and abrupt effects, have been detected as well [5–9]. There are more than 700 kinds of Chlorination disinfection by-products which have been detected in drinking water and that are harmful to the human body, including more than 20 kinds of carcinogens and 50 kinds of mutants which threatens the drinking water safety and the health of the people [10–16]. Therefore, the migration and transformation rules of OFL and disinfection by-products in the water environment and their harm to the environment have been of wide concern.

While the degradation of OFL has been investigated in previous research, they mainly focused on the simple reaction environment of the beaker deionized water [4,6,7]. The environment in the pipe networks is much more complex, and research of the degradation, migration and transformation process of OFL in the pipe network has not been reported [13–16]. Therefore, this study investigated the degradation kinetics, migration and transformation mechanism of the OFL in the pipe network and the deionized water under the action of the free chlorine to provide a reference for the effective control of OFL in the urban water system and the protection of the human and living body.

## 2. Materials and Methods

### 2.1. Test Materials and Instruments

A number of test reagents have been used in this study, including sodium hypochlorite, sodium hydroxide, sodium thiosulfate, ascorbic acid, phosphate, disodium hydrogen phosphate, sodium dihydrogen phosphate, boric acid, borax, concentrated hydrochloric acid, residual chlorine powder, methanol, acetonitrile, CNWBOND HC-18 SPE (500 mg/3 mL, CNW Technologies GmbH, Düsseldorf, Germany) extraction column, and methyl tert-butyl ether (MTBE). The test instruments that have been employed for the analysis include Agilent-2100 High Performance Liquid Chromatography (HPLC, Agilent Technologies, Santa Clara, CA, USA), an Agilent-6460 liquid phase triple quadrupole mass spectrometer (LC-MS, Agilent Technologies, Santa Clara, CA, USA), a DR 2800 UV spectrophotometer (Shimadzu, Kyoto, Japan), an NW Ultra-cure system Super pure water machine (Sigma Aldrich, Shanghai, China), a PHS-3C type pH meter (Sigma Aldrich, Shanghai, China), a liquid gun (Sigma Aldrich, Shanghai, China), a CNW-12 type 12-hole solid phase extraction device (Sigma Aldrich, Shanghai, China), an ND-200 type nitrogen sweeper (Sigma Aldrich, Shanghai, China), a magnetic electromagnetic agitator (Reagent Co., Ltd. Shanghai, China), an ultrasound (Reagent Co., Ltd. Shanghai, China), a dry box (Reagent Co., Ltd. Shanghai, China), EL204 electronic analysis scales (Reagent Co., Ltd. Shanghai, China), a storage of refrigerators, and a liquid extraction device (Sigma Aldrich, Shanghai, China). All of these experiments were undertaken in a water quality comprehensive simulation platform of a large pipe network, as illustrated in Figure 1.

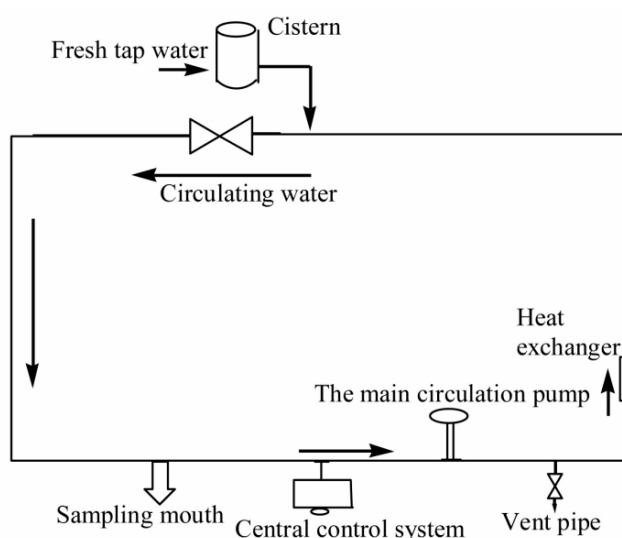


Figure 1. Experimental device for the water distribution system.

### 2.2. Experimental Methods

#### 2.2.1. Decomposition of OFL in the Pipe Network

The experimental platform consists of loops with different materials, including the cement lining of ductile iron, polyethylene (PE) materials and stainless-steel materials. The diameter of all of the

pipes is 150 mm. Before the experiment, the experimental loop and the drug pump were washed with fresh tap water for about 30 min, and the water was drained after cleaning. After that, the fresh tap water was injected again to start the experiment. The experimental parameters such as the flow rate and water temperature were adjusted to the set value through the central control system. In the experiment that needs to adjust the pH of the water body, the solution pH was adjusted by adding the appropriate sodium hypochlorite or NaOH solution to the pipe network using a drug pump according to the experimental conditions. When all of the experimental conditions reach the set value, a certain amount of sodium hypochlorite solution was added. After the residual chlorine reached the desired value, the formulated and fully dissolved OFL solution was added to make the concentration of OFL in the pipe network be 250 µg/L. After the solution was added to the pipe network, 250 mL brown glass bottles were used for sampling at different reaction times, and the appropriate amount of Na<sub>2</sub>S<sub>2</sub>O<sub>3</sub> was added immediately to terminate the experiment. The concentration of OFL at different times was measured by HPLC at the end of the experiment. We note that while the real OFL concentration can be significantly lower than the concentration (250 µg/L) used in this study, the underlying mechanism/properties of the OFL revealed in this study can be used as guidance to control/manage the OFL in the real water supply system with low concentrations.

### 2.2.2. Degradation of OFL in Beaker Deionized Water

The appropriate amount of deionized water was added to the 250 mL conical bottle, and the appropriate amount of phosphoric acid or NaOH solution was added to adjust the pH. After that, the NaClO reserve liquid was added to reach the residual chlorine requirement. Finally, the OFL reserve liquid was added to start the reaction. At different reaction times, a 1 mL sample was added to a brown reagent flask, prior to which 2.0 mL Agilent with 0.1 mL Na<sub>2</sub>S<sub>2</sub>O<sub>3</sub> was already added into the flask. The concentration of OFL was measured using HPLC.

## 2.3. Analytical Methods

### 2.3.1. The Analysis Method of Chlorine and OFL

A *N,N*-diethyl-1,4-phenylenediamine sulfate (DPD) spectrophotometry was used with the DR-2800 spectrophotometer (HACH, Loveland, CO, USA) to measure the concentration of chlorine at a detection wavelength of 530 nm. The concentration of OFL was monitored by an Agilent 1200 high performance liquid chromatography (HPLC) system (Agilent Technologies, Santa Clara, CA, USA) with a UV detector (Shimadzu, Kyoto, Japan) at 293 nm. The separate column was the Zorbax Eclipse XDB-C18 column (4.6 mm × 150 mm, 5 µm particle size) with a column temperature of 30 °C. A mixture of 0.1% formic acid/acetonitrile (75/25, *v/v*) was used as eluents at the flow rate of 1.0 mL/min and the injection volume of 50 µL.

### 2.3.2. LC-MS Analysis Method of OFL Chlorination Products

The chlorination products of OFL were analyzed by the solid phase extraction-liquid chromatography-mass spectrometry (SPE-LC-MS) technique. Before the solid phase extraction, 1 L samples were filtered by an ultrafiltration membrane with an aperture of 0.45 µm to remove large particles. The hydrophilic lipophilic balanced (HLB) extraction cartridges were activated by adding 6 mL and 10 mL of pure water in an orderly way. Next, 1 L samples were loaded into activated cartridges at a flow rate of 5 mL/min. 6 mL methanol was used to elute OFL and its chlorination byproducts, and then the extracts were concentrated to a final volume of 0.1 mL with a gentle nitrogen stream. Finally, the OFL and its intermediates were analyzed by electrospray ionization/liquid chromatograph/mass spectrometry (ESI+/LC/MS) (Agilent 6460, Varian, Palo Alto, CA, USA). A Zorbax SB-18 capillary column with a particle size of 5 µm (2.4 mm × 150 mm, 5 µm) was used. The mobile phase at a flow rate of 0.3 mL/min with 0.2% formic acid (A) and acetonitrile (B) was used. The elution gradient was: 20% B for 5 min, then increased to 35% B over 10 min, followed by a change to 80% B over

5 min, before being finally increased to 100% B over 3 min. An ESI source in positive ion modes with the mass range of the total ion-current (TIC) from 50 to 500 was used in the mass spectrometer analysis. The carrier gas temperature of the ionization conditions of the source was 350 °C. The pressure was 25 psig, theragenerator voltage was 110 eV, and the capillarity voltage was 4000 V.

### 2.3.3. The Analytical Method for THMs and HAAs

The liquid extraction was conducted for the pretreatment of the water sample before the analysis of THMs and HAAs. The sample was then placed in a 40 mL glass bottle, and 2 mL MTBE and 8 g anhydrous Na<sub>2</sub>S<sub>2</sub>O<sub>4</sub> were added. The bottle was shocked to dissolve Na<sub>2</sub>S<sub>2</sub>O<sub>4</sub> and was then set for 30 min. After that, 0.2 mL of the upper liquid was extracted into a brown chromatograph bottle for analysis.

Gas chromatography with an electron capture detector (GC-ECD) (GC-450, Varian, Palo Alto, CA, USA) was used to detect the concentration of THMs during the OFL chlorination. An Agilent DB-5 capillary column (30 m × 0.25 mm × 0.25 μm) (Agilent Technologies, Santa Clara, CA, USA) with a flow of 1 mL/min was used in the test. A splitless injection was used at 150 °C in the injectors. The temperature program of the ECD detector was 1 min at 50 °C, before being increased at 20 °C/min to 250 °C.

For the HAA detection, the samples were first derivatized with methyl tert-butyl ether (MTBE). GC (GC-450, Varian, Palo Alto, CA, USA) with an Agilent HP-5 capillary column (15 m × 0.25 mm × 0.25 μm, Agilent Technologies, Santa Clara, CA, USA) was used in the HAAs detection. A headspace injection with a temperature of 175 °C in the injectors was used. The temperature of the detector was 300 °C and the column flow was 1 mL/min. The temperature program was 5 min at 40 °C, increased by 10 °C/min to 140 °C, and then increased by 25 °C/min to 190 °C, and held for 3 min.

## 3. Results and Analysis

### 3.1. Kinetics of the Degradation of OFL by Free Chlorine

#### 3.1.1. Degradation of OFL at Different Free Chlorine Concentrations

The test conditions were: the pH was 7.4, the reaction temperature was 20 °C, the pipe material was PE (PE pipe material has been widely used in China, especially for relatively small diameters, due to its low cost and great ability to prevent corrosion), the flow rate was 1 m/s, the initial concentration of OFL was 250 μg/L, and the initial concentrations of free chlorine were 0.3 mg/L, 0.7 mg/L, 1.0 mg/L and 1.3 mg/L, respectively.

As can be seen from Figure 2a,b, the concentration of OFL gradually decreases with the increase of the reaction time. One can see that the effect of the initial total free chlorine concentration on the degradation of OFL is significant both in the pipe network and deionized water. When the free chlorine concentration is 0.7 mg/L, 1.0 mg/L and 1.3 mg/L, the removal rate of OFL can reach more than 90% after 5 min in the pipe network, while the removal rate can only reach 80% at a free chlorine concentration of 0.3 mg/L. After a 10 min reaction time, when the initial total free chlorine concentration increased from 0.3 mg/L to 1.3 mg/L, the removal rates were 91.7%, 96.8%, 100%, and 100%. In the deionized water, the removal rate of OFL reaches 100% at 3 min when the concentration is 1.3 mg/L. When the initial total free chlorine concentration increased from 0.3 mg/L to 1.3 mg/L, the removal rate was 94.5%, 100%, 100%, and 100%. The comparison shows that the degradation rate of OFL in the deionized water is higher than that in the pipe network. The rationale behind this finding is that organic matter, pipe scale and biofilm in the pipe network consume part of the free chlorine, which reduces the proportion of total free chlorine used for the degradation of OFL in the pipe network.

The experimental data obtained from the degradation of OFL in deionized water at different free chlorine concentrations were fitted with the pseudo first-order reaction Kinetics equation, with results shown in Figure 3. One can see that the linear relationship between  $\ln[C/C_0]$  and the reaction time is

strong. This indicates that the reaction of the OFL chlorination by free chlorine (OFC) is a first-order reaction. Figure 4 shows that a strong linear relationship can be observed between the pseudo first-order reaction rate constant ( $k_{obs}$ ) and the free chlorine concentration, indicating that the reaction between the free chlorine concentration and OFL conforms to the second-order kinetic model.  $k_{obs}$  is the slope obtained by the linear fitting  $\ln[C/C_0]$  and the reaction time T, and a larger  $k_{obs}$  value indicates a faster reaction rate.

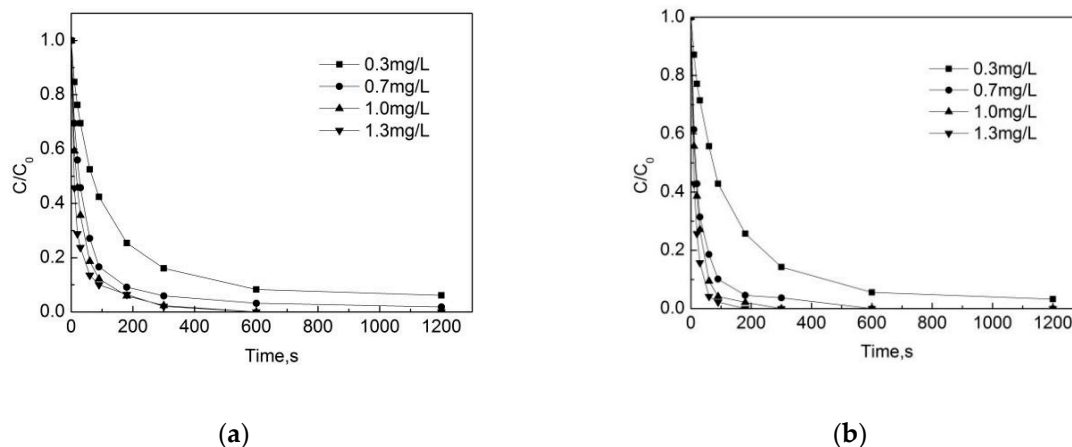


**Figure 2.** Degradation of Ofloxacin (OFL) under different free chlorine concentrations in (a) the water distribution system and in (b) deionized water. [C] represents the concentration of OFL at different reaction times, and  $[C_0]$  represents the initial OFL concentration.

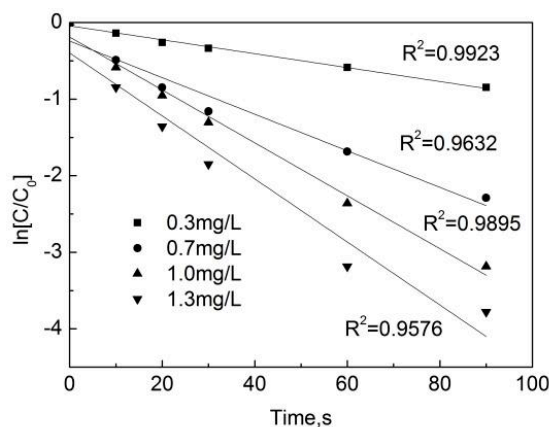


**Figure 3.** Dynamic fitting curves of OFL under different free chlorine concentrations in deionized water.

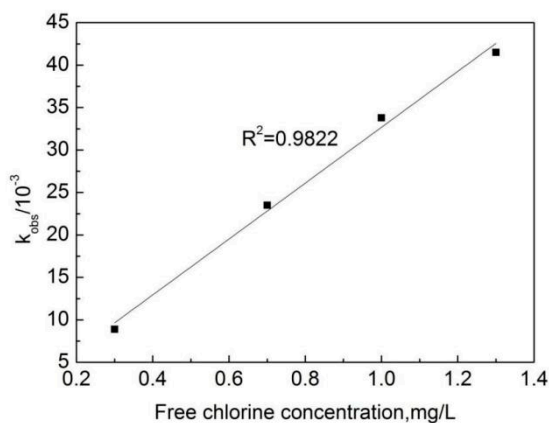
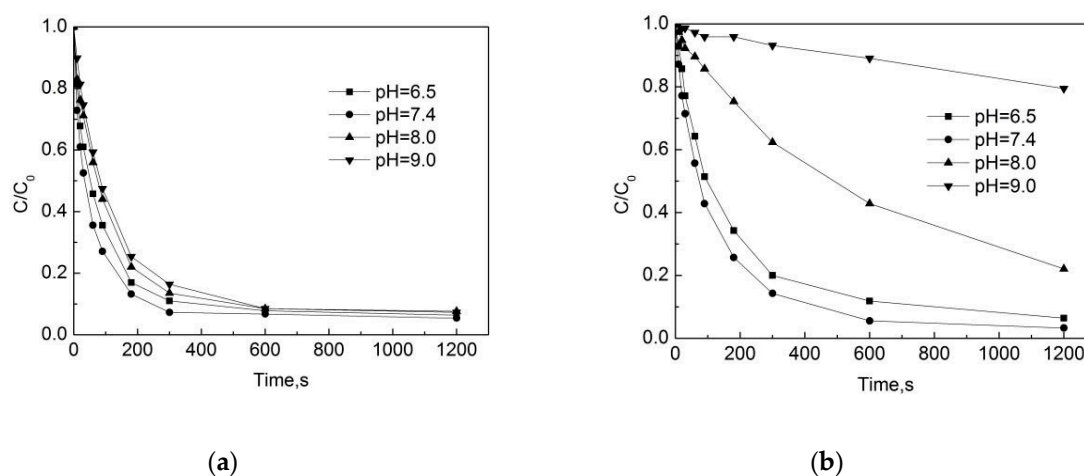


**Figure 4.** The relation curve between the effective free chlorine concentration and  $k_{obs}$ .

### 3.1.2. Degradation of OFL at Different pH Conditions

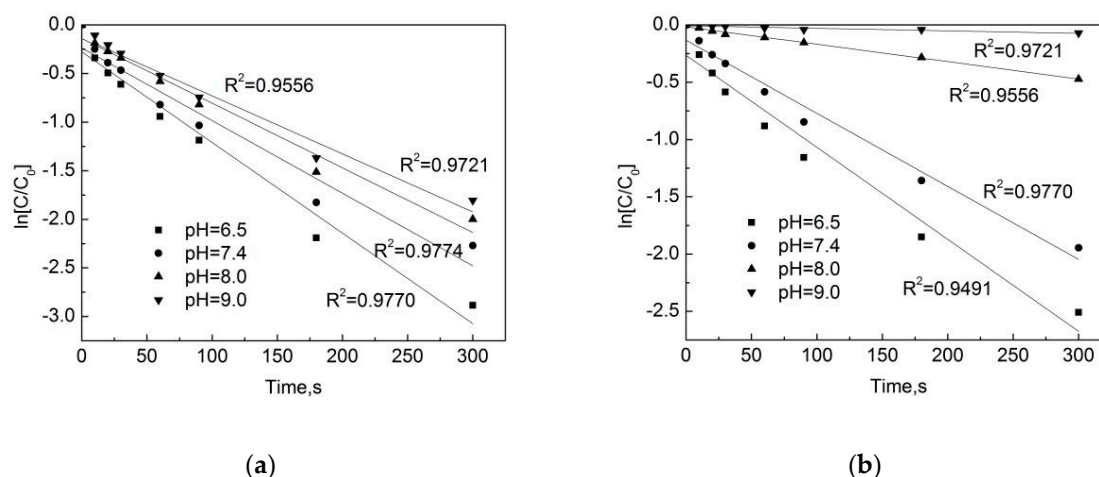
Test conditions: the initial free chlorine concentration was 0.3 mg/L, the initial pipe network concentration of OFL was 250  $\mu\text{g/L}$ , the pipe material was PE, the pipe flow rate was 1 m/s, the temperature was 20  $^{\circ}\text{C}$ , and the degradation of OFL in both the beaker deionized water and in the PE pipe were investigated.

Figure 5a,b shows that the degradation rate of OFL is the fastest under neutral conditions, and that the relative removal efficiency is relatively low under acidic conditions, followed by the lowest rate under alkaline conditions. In the pipe network, after the reaction of 5 min, the removal rates of OFL are 89%, 92.7%, 86.5% and 83.6% at pHs of 6.5, 7.4, 8.0, and 9.0, respectively. In the deionized water, the removal rates of OFL were 80%, 85.7%, 37.7%, and 6.9% at pHs of 6.5, 7.4, 8.0, and 9.0, respectively. One can see that the pH value has a significant effect on the OOFc, and that the degradation rate of OFL in the pipe network is faster than in the deionized water. This may be due to some substances in the water and pipe scale that can promote the degradation of the OFL chlorination. When  $\text{pH} \leq 7.4$ , both the degradation rate of OFL in the pipe network and in the deionized water are faster. When  $\text{pH} = 7.4$ , the removal efficiency of OFL is the highest, while at  $\text{pH} = 9.0$  the removal efficiency of OFL is the lowest. This is because the pH has a combined effect on the presence of sodium hypochlorite and the presence of OFL. The OFL is an amphoteric compound, and the OFL has a different dissociation in water in different pH conditions. The OFL mainly exists in the form of  $\text{OFL}^+$  under acidic conditions, in the form of  $\text{OFL}^0$  under neutral conditions, and in the form of  $\text{OFL}^-$  under alkaline conditions. When the pH is 6.5 and 7.4, the chlorination reaction rate is mainly determined by hypochlorous acid (HOCl) and OFL. When the pH is higher than 7.4 and the concentration of HOCl decreases, the main participation in the reaction is  $\text{ClO}^-$ . As the  $\text{ClO}^-$  chlorination is weaker than HOCl [17], the reaction rate is reduced.



**Figure 5.** Degradation of OFL under different pH in (a) water distribution system; (b) deionized water.

As shown in Figure 6, in the pipe network, when the pH is 7.4, the pseudo first-order rate constant is the highest, with a  $k_{\text{obs}} = 0.0084 \text{ s}^{-1}$ , and when the pH is 9.0 the pseudo first-order rate constant is the lowest, with a  $k_{\text{obs}} = 0.0061 \text{ s}^{-1}$ . In the deionized water, when the pH is 7.4 the pseudo first-order rate constant is the highest, at  $k_{\text{obs}} = 0.0048 \text{ s}^{-1}$ , and when the pH is 9.0 the pseudo first-order rate constant is the lowest, at  $k_{\text{obs}} = 0.0002 \text{ s}^{-1}$ . One can see that there is a significant difference in the degradation rate of OFL chlorination under different pH conditions in the pipe network and deionized water, and the difference in degradation is even greater under alkaline conditions. This is because as the increase of pH, substances in water and pipe scale can promote the degradation of OFL.



**Figure 6.** Dynamic fitting curves of OFL under different pHs in (a) the water distribution system, and in (b) the deionized water.

### 3.1.3. Degradation of OFL under Different Pipe Conditions

Test conditions: the initial free chlorine concentration was 0.3 mg/L, the initial OFL concentration in the pipe network was 250  $\mu\text{g/L}$ , the pipe flow rate was 1 m/s, the temperature was 20  $^{\circ}\text{C}$ , the pH was 7.4, and the pipe types included ductile iron pipes, stainless steel pipes and PE pipes. The results are shown in Figure 7.

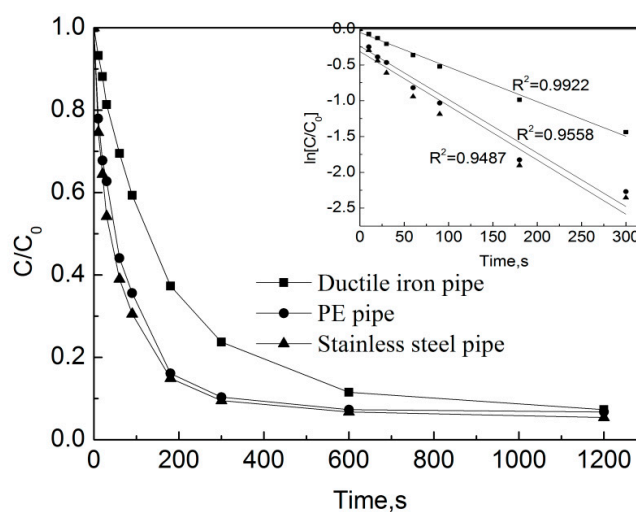


**Figure 7.** Degradation of OFL under different pipe materials in the water distribution system.

Figure 7 shows that after the reaction of 3 min, the removal rates of OFL in the ductile iron pipes, PE and stainless-steel pipes were 62.9%, 83.9%, and 85.1%, respectively. After the reaction of 20 min, the removal rates of OFL in the ductile iron pipes, PE and stainless-steel pipes were 92.7%, 93.2% and 94.6%, respectively. The pseudo first-order rate constants of OFL in the ductile iron pipes, PE and stainless-steel pipes are  $k_{\text{obs}} = 0.0048 \text{ s}^{-1}$ ,  $0.0075 \text{ s}^{-1}$  and  $0.0076 \text{ s}^{-1}$ , respectively. One can see that the degradation rate of OFL in the ductile iron pipes is the slowest, while the rate of degradation in the PE pipes is similar to that in the stainless-steel pipes. By observing the visual pipe segment within the pipe network (i.e., the transparent segment of each pipe), the pipe scale in the stainless-steel pipe network is the highest, followed by the PE pipe, and the ductile iron pipe is the lowest. The analysis of the water in the three pipe networks shows that there is a small amount of iron ions in the water of the stainless-steel pipe network. According to the previous study [18],  $\text{Fe}^{2+}$  could react with free chlorine to produce  $\text{Fe}^{3+}$ , and the chlorination process produces some free radicals [19]. This might be

one reason that results in a faster degradation of OFL in the stainless-steel pipe compared to the one in the other two pipes. By considering the effect of iron ions and the pipe scale, the degradation rate of OFL in the PE pipes is approximately equal to that in the stainless-steel pipes, while that in the ductile cast iron pipe network is the slowest.

### 3.1.4. Degradation of OFL at Different Flow Rates

Since the effect of different flow rates on the degradation of OFL is only present in the pipe network, the PE pipes were chosen and the degradation in the deionized water is not considered. Therefore, in order to study the effect of different flow rates on the degradation of OFL, the initial free chlorine concentration was 0.3 mg/L, the concentration of OFL in the initial pipe network was 250 µg/L, the temperature was 20 °C, the pH of the pipe network was 7.4, and the flow rates were 0.5 m/s, 1.0 m/s, and 1.5 m/s.

Figure 8 indicates that the degradation rate of OFL in the pipe network with the flow rate of 1.0 m/s is the fastest, while that in the pipe network with the flow rate of 1.5 m/s is the slowest. The removal rate of OFL was 90.8%, 89.0% and 87.8% at the flow rates of 1.0 m/s, 1.5 m/s and 1.0 m/s, respectively. The effect of the increase in the flow rate on the reaction rate is not obvious. According to hydraulics knowledge, when the speed is 0.5 m/s, the Reynolds number is higher than 2300 and the water is already in turbulent state. When the flow rate increases from 0.5 m/s to 1.5 m/s, the material exchange is sufficient, and hence the effect of the increase of the flow rate on the degradation rate of OFL is insignificant.

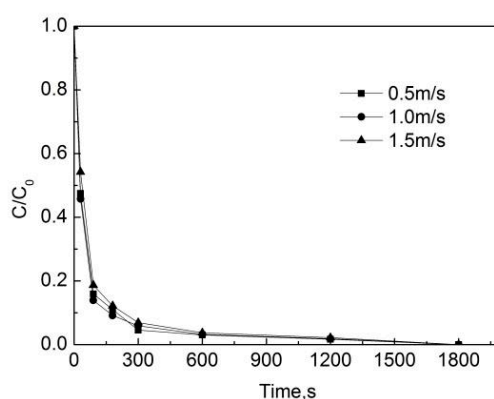


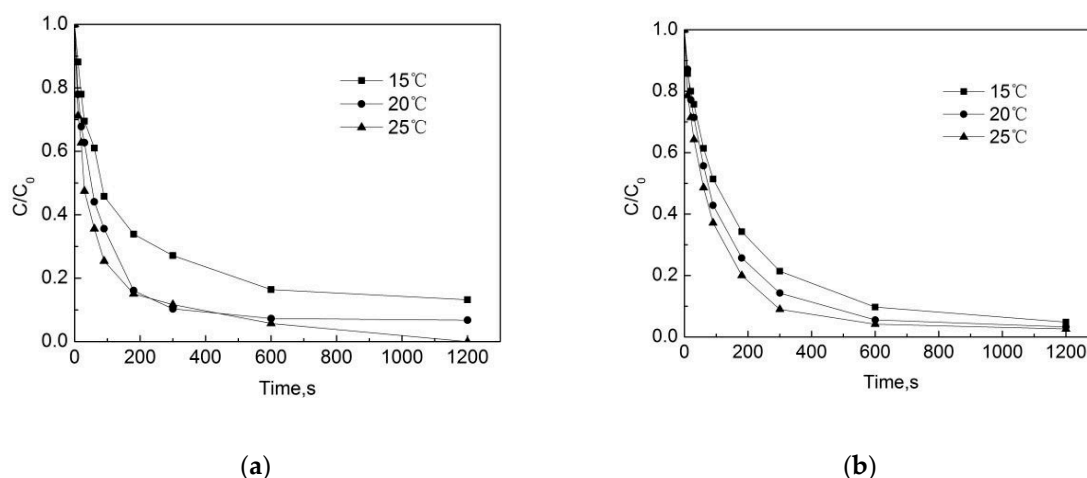
Figure 8. Degradation of OFL under different flow rates in the water distribution system.

### 3.1.5. Degradation of OFL at Different Temperatures

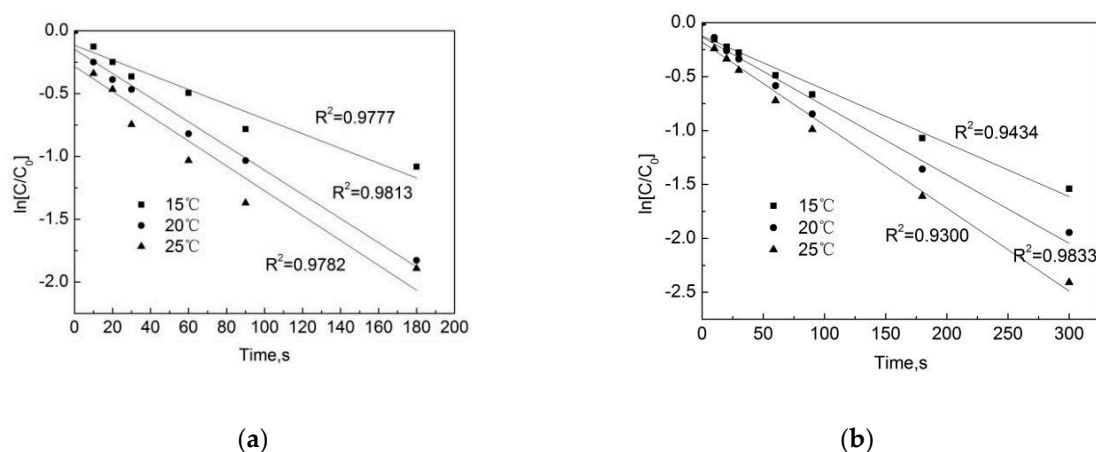
Test conditions: the initial free chlorine concentration was 0.3 mg/L, the initial pipe network concentration of OFL was 250 µg/L, the pipe material was PE, the pipe flow rate was 1 m/s, the pH of the water in the pipe network was 7.4, and the temperatures were 15 °C, 20 °C and 25 °C. The results are shown in Figure 9.

Figure 9 shows that the temperature has a significant effect on the degradation of OFL both in the pipe network and in the deionized water. The degradation rate continues to rise as the temperature increases from 15 °C to 20 °C. After 90 s, the removal rates of OFL in the pipe network were 48.6%, 57.2%, and 63.9%, and those in the deionized water were 54.2%, 64.4%, and 74.6%. As shown in Figure 10, as the temperature increases, the degradation rate in both conditions increases. This is because, when the temperature rises, the average kinetic energy and activation molecular weight of the molecule in the reaction system will increase, resulting in an increase in the number of effective collisions of molecules during the reaction process, as a result of which the chlorination reaction rate will be accelerated. However, we also note that at the same temperature, the degradation rate of OFL in the pipe network is slightly lower than that in the deionized water. In the pipe network, when the reaction temperature rises from 15 °C to 25 °C, the degradation rate of OFL increases from 0.0057 s<sup>-1</sup>

to  $0.0085\text{ s}^{-1}$ , while it rises from  $0.0059\text{ s}^{-1}$  to  $0.0099\text{ s}^{-1}$  in the deionized water. This is due to the water organic matter, pipe scale, and pipe wall microorganisms, which consume a certain amount of free chlorine and reduce the free chlorine for the OFL chlorination.



**Figure 9.** Degradation of OFL under different temperatures in (a) the water distribution system, and in (b) the deionized water.



**Figure 10.** Dynamic fitting curves of OFL under different temperatures in (a) the water distribution system, and in (b) the deionized water.

To find out the effect of the temperature on the reaction,  $\ln k$  and  $1/T$  were fitted according to the Arrhenius equation, and the results are shown in Figure 11. According to the Arrhenius equation:

$$\ln k = -\frac{Ea}{RT} + \ln A \tag{1}$$

where  $A$  is the frequency factor,  $Ea$  is the reaction activation energy,  $R$  is the gas general constant with a value of  $8.314$ , and  $T$  is the thermodynamic temperature. According to the equation and the slope of the fitting line, the reaction activation energy of the OOFC in the pipe network is  $37.04\text{ kJ/mol}$ , while it is  $28.63\text{ kJ/mol}$  in the deionized water. This means that the degradation of OFL in the deionized water is more likely to occur.

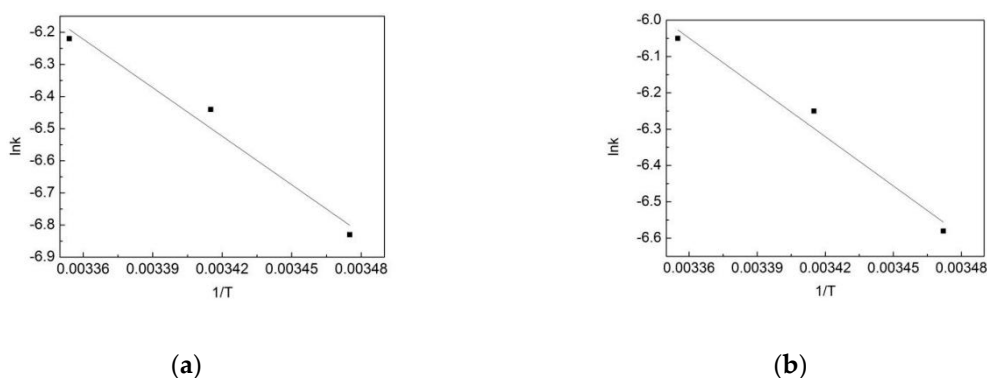


**Figure 11.** Arrhenius fitting of OFL chlorination by free chlorine (OFC) in (a) the water distribution system, and in (b) the deionized water.

### 3.2. Analysis of the Production Law of Intermediary Products.

During the intermediate product analysis, the experimental conditions are as follows: the pipe material was PE, the flow rate was 1.0 m/s, the temperature was 20 °C, the pH was 7.4, the initial free chlorine concentration was 0.3 mg/L, and the initial OFL concentration was 250 µg/L. At 0 h, 15 min, 1 h, 3 h, 6 h and 24 h after the experiment started, a 1 L sample was added to the glass bottle respectively and 2 g of  $\text{Na}_2\text{S}_2\text{O}_4$  were added immediately to terminate the experiment. The results of the chromatogram at reaction times of 0 h and 24 h are shown in Figure 12, and the mass spectrogram of the products is given in Figure 13. Based on the information presented in Figure 13, the mass-charge ratio and molecular weight of the main products are derived as shown in Table 1. The potential degradation path is derived as given in Figure 14, with a detailed analysis given below.

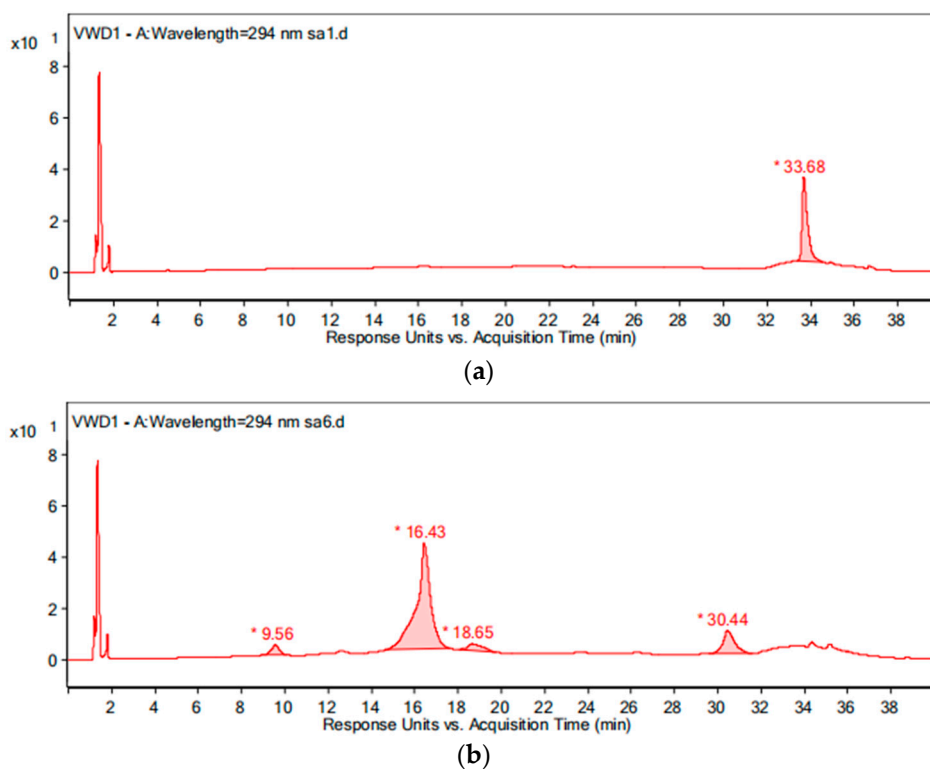


**Figure 12.** The chromatogram of the water sample at reaction times of: (a) 0 h and (b) 24 h.

By comparing with the 0 h water sample, one can see that the reaction has a relatively obvious fragmentation peak at 16.45 min, 18.67 min, and 30.42 min. By comparison, one can see that the fragment ion can be found at 15 min, 1 h, 3 h, 6 h and 24 h and that the molecular weight is 261.1. At the beginning of the reaction (Figure 14), the fragment ions attack the hydroxyl group on the piperazine ring, seize the hydrogen and lose one H<sub>2</sub>O molecule to form the chlorination product M-18 (the charge-to-charge ratio is 345.2), also losing a CO<sub>2</sub> molecule to form the chlorination product M-44 (mass ratio is 318).

After further analysis of its chlorination products, it is found that the piperazine ring is one of the main groups involved in the reaction, and the main point involved in the chlorination reaction is the N4 atom on the piperazine ring. It loses one-CH<sub>3</sub> to form the chlorination product M-61 (the mass ratio is 301), continues to act on the N4 atom on the piperazine ring, and removes C<sub>3</sub>H<sub>7</sub>N to form the chlorination product M-101 (the mass ratio is 261.1). The chlorination product M-139 is formed by the ring opening of oxazine (the charge ratio is 223.1). The N2 atom on the quinolone ring is replaced by Cl to form the chlorination product M-108 (the charge-to-charge ratio is 254.1).

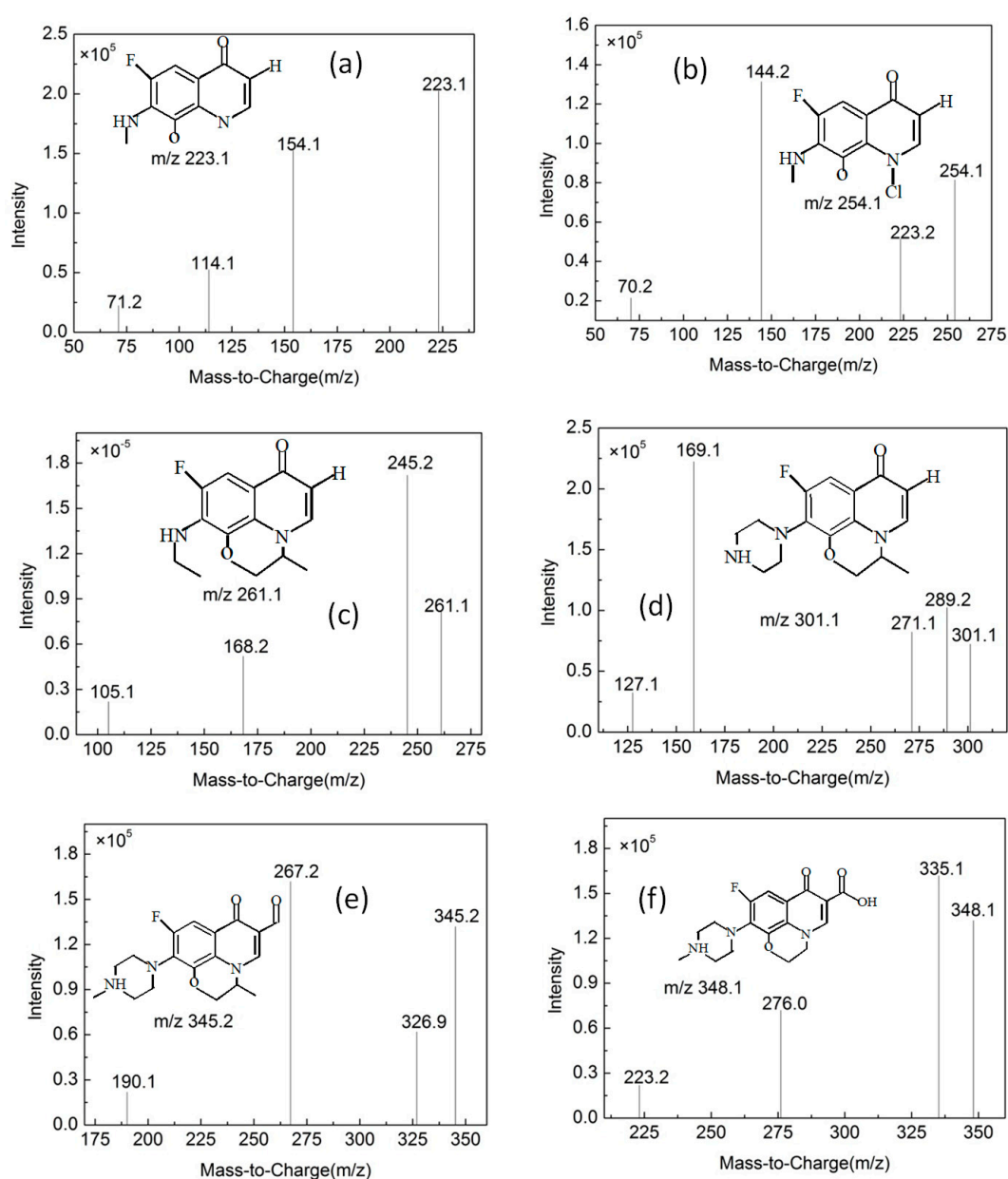


Figure 13. Mass spectrogram of the products (for details see Table 1).



### 3.3. Analysis of the Formation Law of THMs and HAAs

The experimental conditions are as follows: the pipe material was PE, the flow rate was 1.0 m/s, the temperature was 20 °C, the pH was 7.4, the initial free chlorine concentration was 0.3 mg/L, and the initial OFL concentration was 250 µg/L. At 0 h, 15 min, 1 h, 3 h, 6 h, and 24 h, a 200 mL sample was taken into the glass bottle respectively, and 1 g of Na<sub>2</sub>S<sub>2</sub>O<sub>4</sub> was immediately added to terminate the experiment. Then, a liquid extraction was used to preprocess the water sample, before a 30 mL sample were placed in a 40 mL glass bottle. After that, 2 mL of MTBE and 8 g of anhydrous Na<sub>2</sub>S<sub>2</sub>O<sub>4</sub> was added, shaking to dissolve Na<sub>2</sub>S<sub>2</sub>O<sub>4</sub>, and the bottle was left for 30 min. Finally, 0.2 mL of the upper liquid was extracted to a brown chromatograph bottle for the analysis.

The formation curves of three kinds of THMs detected in the experiment are shown in Figure 15, which are trichloromethane (TCM), monobromodichloride (DCBM) and dibromodichloride (DBCM). It can be seen that THMs in the raw water mainly exist in the form of TCM. The concentration of three THMs increases significantly with the increase of the reaction time in the first 6 h. After 6 h, the concentration of DCBM and DBCM increases slowly while the concentration of TCM still increases significantly. After 24 h, the concentrations of TCM, DCBM and DBCM are 36.61 µg/L, 27.23 µg/L, and 5.808 µg/L, respectively.

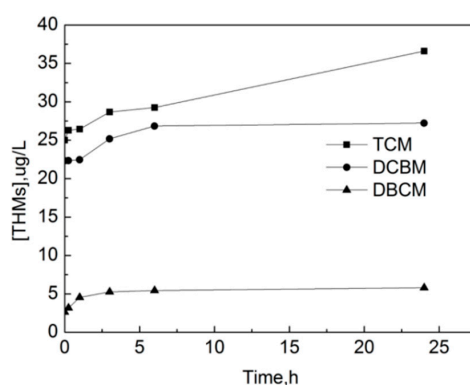


Figure 15. The formation curve of trihalomethanes (THMs) in the process of OOFC.

As can be seen from Figure 16, HAAs in water bodies mainly exist in the form of monochloroacetic acid (MCAA). After the reaction begins, the concentration of free chlorine in the pipe network is relatively high, the free chlorine components used for the reaction with OFL are sufficient and the concentration of three HAAs gradually increases with the increase of the reaction time. The increase of MCAA is particularly obvious, and the increase of monobromoacetic acid (MBAA) and dichloroacetic acid (DCAA) are subsequently stable. The rate of the production of MCAA is the fastest in the first 6 h, and due to the continuous consumption of free chlorine the rate of production decreases later. After 24 h, the concentrations of MCAA, MBAA and DCAA are 1.32 µg/L, 0.23 µg/L, and 0.08 µg/L, respectively.

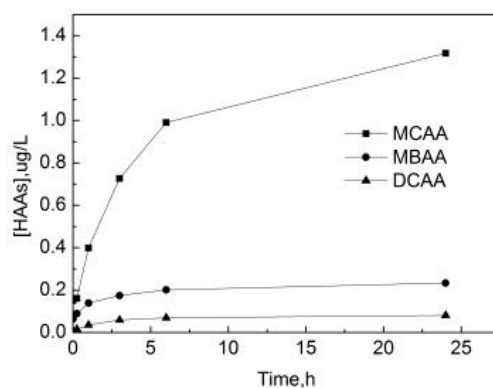


Figure 16. The formation curve of haloacetic acids (HAAs) in the process of OOFC.

#### 4. Conclusion

1. The reaction rate of OFL in the pipe networks and deionized water increases with the increase of the free chlorine concentration and temperature. The degradation rate of OFL under the neutral conditions is the fastest. The removal efficiency is lower under acidic conditions, and the removal efficiency is the lowest under alkaline conditions.
2. The degradation of OFL in the pipe network does not change significantly with the different flow rates, while it is affected by different pipe materials. Under the combined effect of the iron ions and pipe scale, the degradation rate of OFL in the stainless-steel pipe is similar to that in the PE pipe, but both are greater than the ductile cast iron pipe.
3. As the reaction time increases, the concentrations of THMs and HAAs will gradually increase. THMs mainly exist in the form of TCM, and HAAs mainly exist in the form of MCAA.
4. Further analysis of the intermediate chlorination product shows that the piperazine ring is one of the main groups involved in the reaction, and that the main point involved in the chlorination reaction is the N4 atom on the piperazine ring, which is mainly responsible for dealkylation and hydroxylation, and which produces intermediate chlorination products.

**Author Contributions:** Writing—original draft, review and editing, W.B.; data collection, formal analysis, investigation and methodology, Y.J.; supervision, H.W.

**Funding:** This research was funded by National Natural Science Foundation of China, grand number 51808497 and Zhejiang Provincial Department of Education General Research Foundation (Natural Science), grand number Y201636517.

**Conflicts of Interest:** The authors declare no conflict of interest.

#### References

1. Janecko, N.; Pokludova, L.; Blahova, J.; Svobodova, Z.; Literak, I. Implications of fluoroquinolone contamination for the aquatic environment—A review. *Environ. Toxicol. Chem.* **2016**, *35*, 2647–2656. [[CrossRef](#)] [[PubMed](#)]
2. Snowberger, S.; Adejumo, H.; He, K.; Mangalgiri, K.P.; Hopanna, M.; Soares, A.D.; Blaney, L. Direct photolysis of fluoroquinolone antibiotics at 253.7 nm: Specific reaction kinetics and formation of equally potent fluoroquinolone antibiotics. *Environ. Sci. Technol.* **2016**, *50*, 9533–9542. [[CrossRef](#)] [[PubMed](#)]
3. Serna-Galvis, E.A.; Berrio-Perlaza, K.E.; Torres-Palma, R.A. Electrochemical treatment of penicillin, cephalosporin, and fluoroquinolone antibiotics via active chlorine: Evaluation of antimicrobial activity, toxicity, matrix, and their correlation with the degradation pathways. *Environ. Sci. Pollut. Res.* **2017**, *24*, 23771–23782. [[CrossRef](#)] [[PubMed](#)]
4. El Najjar, N.H.; Deborde, M.; Journal, R.; Leitner, N.K. Aqueous chlorination of levofloxacin: Kinetic and mechanistic study, transformation product identification and toxicity. *Water Res.* **2013**, *47*, 121–129. [[CrossRef](#)] [[PubMed](#)]
5. Liu, X.; Wang, Z.; Wang, X.L.; Li, Z.; Yang, C.; Li, E.H.; Wei, M.H. Status of antibiotic contamination and ecological risks assessment in Chinese Several typical surface-water environment. *Environ. Sci.* **2019**, *5*, 1–13. (In Chinese)
6. Wang, X.; Li, Y.; Li, R.; Yang, H.; Zhou, B.; Wang, X.; Xie, Y. Comparison of chlorination behaviors between norfloxacin and ofloxacin: Reaction kinetics, oxidation products and reaction pathways. *Chemosphere* **2019**, *215*, 124–132. [[CrossRef](#)] [[PubMed](#)]
7. Yassine, M.H.; Rifai, A.; Hoteit, M.; Mazellier, P. Study of the degradation process of ofloxacin with free chlorine by using ESI-LCMSMS: Kinetic study, by-products formation pathways and fragmentation mechanisms. *Chemosphere* **2017**, *189*, 46–54. [[CrossRef](#)] [[PubMed](#)]
8. Zhu, L.; Santiago-Schübel, B.; Xiao, H.; Hollert, H.; Kueppers, S. Electrochemical oxidation of fluoroquinolone antibiotics: Mechanism, residual antibacterial activity and toxicity change. *Water Res.* **2016**, *102*, 52–62. [[CrossRef](#)] [[PubMed](#)]

9. Ding, C.S.; Zou, B.W.; Miao, J.; Fu, Y.P.; Shen, J.C. Formation process of nitrogenous disinfection byproduct trichloronitromethane in drinking water and its influencing factors. *Environ. Sci.* **2013**, *34*, 3113–3118. (In Chinese)
10. Tay, K.S.; Madehi, N. Ozonation of ofloxacin in water: By-products, degradation pathway and ecotoxicity assessment. *Sci. Total Environ.* **2015**, *520*, 23–31. [[CrossRef](#)] [[PubMed](#)]
11. Lin, Y.Z.; Liu, X.Y. Research progress of chlorination and disinfection by-products in drinking water. *China Resour. Compr. Util.* **2017**, *35*, 128–130. (In Chinese)
12. Frade, V.M.; Dias, M.; Teixeira, A.C.; Palma, M.S. Environmental contamination by fluoroquinolones. *Braz. Pharm. Sci.* **2014**, *50*, 41–54. [[CrossRef](#)]
13. Zhang, Q.; Zheng, F.; Duan, H.-F.; Jia, Y.; Zhang, T.; Guo, X. Efficient numerical approach for simultaneous calibration of pipe roughness coefficients and nodal demands for water distribution systems. *J. Water Resour. Plan. Manag.* **2018**, *144*, 04018063. [[CrossRef](#)]
14. Qi, Z.; Zheng, F.; Guo, D.; Maier, H.R.; Zhang, T.; Yu, T.; Shao, Y. Better understanding of the capacity of pressure sensor systems to detect pipe burst within water distribution networks. *J. Water Resour. Plan. Manag.* **2018**, *144*, 04018035. [[CrossRef](#)]
15. Qi, Z.; Zheng, F.; Guo, D.; Zhang, T.; Shao, Y.; Yu, T.; Zhang, K.; Maier, H.R. A Comprehensive framework to evaluate hydraulic and water quality impacts of pipe breaks on water distribution systems. *Water Resour. Res.* **2018**, *54*, 8174–8195. [[CrossRef](#)]
16. Zheng, F.; Zecchin, A.C.; Newman, J.P.; Maier, H.R.; Dandy, G.C. An adaptive convergence-trajectory controlled ant colony optimization algorithm with application to water distribution system design problems. *IEEE Trans. Evol. Comput.* **2017**, *21*, 773–791. [[CrossRef](#)]
17. Zhang, S.; Wang, X.; Yang, H.; Xie, Y.F. Chlorination of oxybenzone: Kinetics, transformation, disinfection byproducts formation, and genotoxicity changes. *Chemosphere* **2016**, *154*, 521–527. [[CrossRef](#)] [[PubMed](#)]
18. Pérez-Moya, M.; Graells, M.; Castells, G.; Amigó, J.; Ortega, E.; Buhigas, G.; Pérez, L.M.; Mansilla, H.D. Characterization of the degradation performance of the sulfamethazine antibiotic by photo-Fenton process. *Water Res.* **2010**, *44*, 2533–2540. [[CrossRef](#)] [[PubMed](#)]
19. Li, C.; Wang, Z.; Yang, Y.J.; Liu, J.; Mao, X.; Zhang, Y. Transformation of bisphenol in water distribution systems: A pilot-scale study. *Chemosphere* **2015**, *125*, 86–93. [[CrossRef](#)] [[PubMed](#)]



© 2019 by the authors. Licensee MDPI, Basel, Switzerland. This article is an open access article distributed under the terms and conditions of the Creative Commons Attribution (CC BY) license (<http://creativecommons.org/licenses/by/4.0/>).